El-Adl Rabeih / Engineering Research Journal 180 (Decamber2023) MD1-MD12

Experimental Analysis of the Contact Phenomenon in a Simulated Drill-string

Gehad A. F. Taher [a], El-Adl Rabeih [a], Heba H. El-Mongy [a, b, *]

[a] *Department of Mechanical Design, Faculty of Engineering- Mataria, Helwan University, Egypt.*

[b] *Centre for Applied Dynamics Research, School of Engineering, University of Aberdeen, UK.*

Abstract

The drill string system is a huge and complex mechanical machine that is used to drill wells for exploring oil and gas. Avoiding the undesired vibrations in the drill string is one of the essential contributions of scientific research. In this paper, an experimental setup is prepared to simulate the contact phenomenon in the drill string system. A G.U.N.T (PT500) fault demonstrator laboratory rig is used to simulate a horizontal drill string system. This study demonstrates the influence of changing operating speed parameter on contact characteristics and lateral vibration response. Experiments show that a very small increase in the operating speed affects the intensity of chaotic response. Moreover, FFT spectra illustrate several sub-harmonic and super harmonic components of the rotor system.

Keywords: Drill string, Contact phenomenon, Lateral vibration, Experimental analysis.

1. Introduction

Drill strings used for drilling oil and gas wells are subjected to severe and unavoidable vibrations that may cause premature failures in the drilling rigs. There are different types of destructive phenomena that may occur in drill strings such as; stick slip, bit bounce, and whirling.

Failures due to drill string vibrations and shock account for 25% of the total nonproductive time per year, in addition of considerable maintenance cost[1].

A drill string consists of a long series of drill pipes and collars, that carries the drilling fluid and transmits torque from the top drive to the downhole section. Due to inevitable eccentricities and asymmetries in the drill pipes and collars, whirling phenomenon may occur in the drill string system especially in its lowest part, i.e. the Bottom Hole Assembly (BHA) [2, 3]. Therefore, a drilling system is usually equipped with Measurement While Drilling (MWD) tools to provide real-time monitoring of the BHA. Therefore, theoretical, and experimental studies are crucial to develop better understanding of the various dynamic phenomena and help in improving field data interpretation [4-6]

A considerable amount of previous literature has focused on the study of lateral vibrations in drill strings. Al-Hiddabi et al. [7] proposed a method to minimize and control the effect of lateral and torsional vibration. De Moraes and Savi [8] investigated a nonlinear mathematical model to study the dynamics of lateral vibration with other destructive vibrations. Xie et al. [1] proposed different dynamic responses of a drill string system with different vibration modes. Extensive studies of drill string vibration have explained more details about undesired vibrations in drill string systems [9-12]. Spanos et al. [13] and Ghasemloonia et al. [14] presented a broad review of the research works on drill string vibration modelling. Previous studies have shown the importance of defining the rate of whirling, the position at which whirling occurs, the kind of whirl, and whether or not drill strings experience contact with borehole wall due to whirling.

Whirling phenomenon in drill strings has two types; forward whirl and backward whirl [15]. The former occurs when the drill pipe whirls around the borehole axis in the same direction of rotation and with its same speed, i.e. leading to surface grazing. The later occurs when the drill pipe whirls in opposite direction to the direction of rotation and with higher speed than the spin speed of the system [9, 16]. This oscillation condition may increase the amplitude of response which leads to high impact with the borehole wall and fatigue of the BHA [17].

Different studies have given a deep insight of the whirling phenomenon and its kinds. Zamani et al. [18] introduced comprehensive reviews of destructive failures in the drill pipe and BHA. Chen et al. [19] discussed the effect of the BHA whirl on the rate of penetration. Kapitaniak et al. [16] estimated the coexistence of forward and backward whirls in the response of the BHA depending on initial conditions and system parameters.

There are numerous studies that involved experimental work to study whirling vibrations and other destructive vibrations in drill strings. Albdiry and Almensory [20] introduced a comprehensive study of drilling failures due to drill string vibrations. Servastava and Teodoriu [21] highlighted the downscaling factors for different parts in drill string system and formulated different designs. Chu and Lu [22] carried out several experiments to explain the influence of operating speed on cntact characteristics. Liao et al. [23] deduced experimentally the values of friction coefficient that cause the drill string to move around the center of a borehole. Liu et al. [24] proposed an experimental technique that aimed to evaluate the suitable weight on bit (WOB) to eliminate lateral vibration. Tian et al. [25] depicted by laboratory test rig the influence of the friction force on the contact phenomenon. Abdo et al. [26] showed experimentally the effect of transverse vibration on fatigue life. Tian et al. [27] represented a new structure of drill string system and showed that the effect of increasing speed was evident.

In this paper, the experimental work is conducted on the test rig to simulate a horizontal drill string system as a Jeffcott rotor. The study demonstrates the contact phenomenon between the drill pipe and the borehole wall due to lateral vibration. Moreover, the effect of increasing running speed on the dynamic response is presented.

2. Experimental Setup

The used experimental test rig is the G.U.N.T ® machinery fault demonstrator (PT 500) located in the Vibration and Dynamics Laboratory of the Faculty of Engineering -Mattaria (see Fig. 1). The machine is designed to measure and analyze the faults that happen in the rotor system. The machine has a variable speed DC motor (0.37 kW) that rotates a uniform stainless-steel shaft through a flexible coupling.

The rotor system is considered as a horizontal BHA that consists of an elastic steel shaft with a rigid disk fixed at the mid span of the shaft. It is supported by two rolling element ball bearings (SKF 6004-2ZR). The vibration signals are picked up through two proximity sensors which are installed in both horizontal and vertical directions, see Fig. 1.

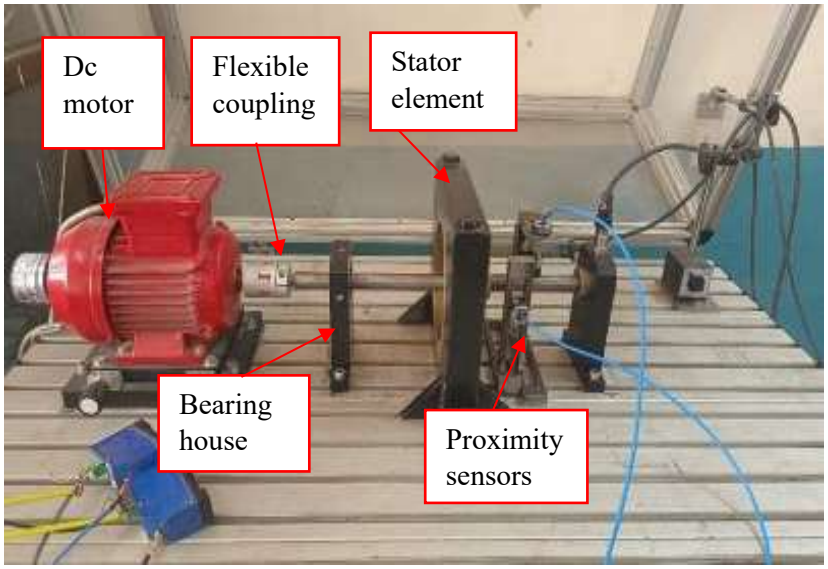

Figure 1 A real picture of the G.U.N.T PT500 fault demonstrator machine.

Table 1 Physical parameters of the G.U.N.T (PT500) fault demonstrator machine.

Description	**Value**	**Description**	**Value**
Disk			
Outer diameter	0.15 m	Mass unbalance	13.2 gm
Inner diameter	0.02 m	Unbalance location	0.06m
Mass of disk	1.52 kg		
Shaft			
Length of shaft	0.44 m	Modulus of elasticity	2.1×10^{11} N/m^2
Damping ratio	0.001	Gravity	9.81 m^2/s
Bearing span	0.3 m	Poisson's ratio	0.3
Bending stiffness	9.3×10^5 N/m	Density	7850 kg/m^3
Coupling			
Type		Inner diameter	0.014 m

	Stepper motor flexible coupling	Length	0.55 m

The stator element is a fixed stator device which represents the borehole wall. The stator is manufactured from steel and copper alloy to reduce the wear with the disk and thermal effect. Table 1 demonstrates the details of the PT-500 machine's components.

The measured signals are analyzed through LabVIEW program. In addition, the sample frequency of the measured signals is 4000 Hz with number of samples equal 16000. The picked-up time is very short to avoid wear and damages during experiments

3. Results and Discussion

In this section, the experimental results aim to study the influence of changing the operating speed on the contact characteristics. The rotor system with rubbing fault exhibits a strong nonlinearity, so the influence of changing the running speed is crucial to study.

The results are represented in form of orbit plot, Poincaré's map, FFT, and time waveform. From previous studies [22, 28], every fault in vibratory systems has a well-known pattern of the orbit plot and Poincare's map. Thus, the graphical plots show clearly the resulted rub fault in the rotor system. The measured vibration signals are in mm in plots, and FFT spectra present in frequency orders.

Hence, Figures 2-6 provide significantly the orbit plots, Poincaré's map, FFT spectra and time waveforms of the rotary system as running speed increases. The critical speed of the rotor system is at 124 Hz.Thus, the operating speed is selected faraway it. The running speeds change from 29 Hz to 51 Hz to indicate the contact characteristics in this range. In this study, the radial clearance is set manually to 0.25 mm and the added mass unbalance is 13.2 g.

Figure 2 show the lateral vibration response when running speed is 29 Hz. It can be noted from time waveforms and orbit plot (see Fig. 2i and 2iii) that there is no contact at this speed. The time waveforms show

irregular sinewave of vibration signal due to noise and misalignment affect the signal. The frequency spectra (Fig. 2iv) also demonstrate 1x harmonic as dominant component.

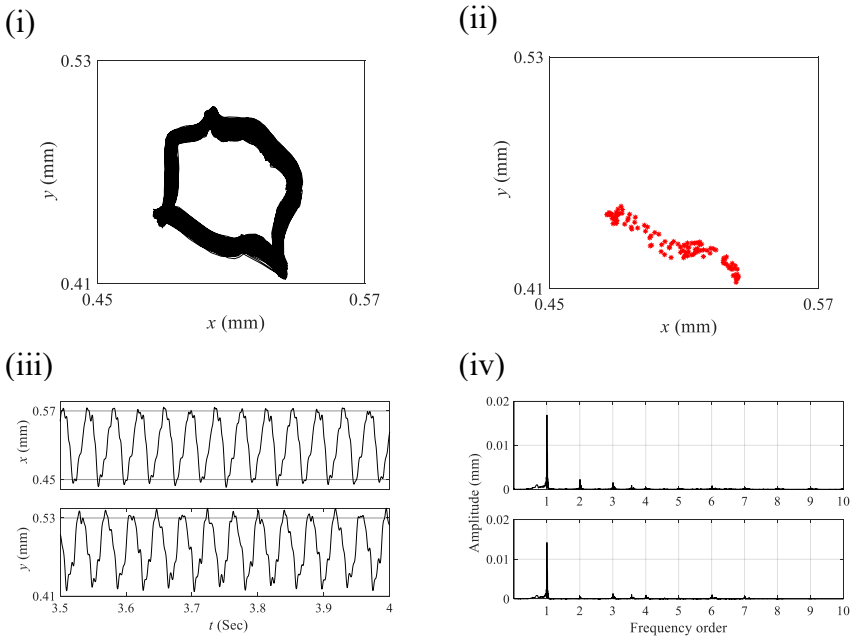

Figure 2 Experimental result of rotating machine at speed 29 Hz; (i) orbit plot, (ii) Poincare's map, (iii) time waveform, and (iv) FFT.

Then when the rotating speed is increased to 37 Hz, the orbit plot and the Poincaré's map (Fig. 3i and 3ii) show that an impact between the rotor and the stator is chaotic in nature. The frequency spectra (see Fig. 3iii) demonstrate super-harmonic components with one fractional harmonic component at 7/2x that appears in the vertical and horizontal direction response. The amplitude of harmonics in the vertical direction is observed to be higher than that in the horizontal direction.

As the speed is become 45 Hz, lateral vibration of the rotor becomes more intense than the previous case (as seen in Fig. 4). The spectra in Fig. 4iii illustrate different harmonic components. Both subharmonic components (5/2x and 7/2x) and super harmonic components up to 5x appear clearly in the spectra. The unique points in the Poincaré's map

(Fig. 4ii) illustrate a random response (attractors). It is noted from observed result that the contact response is chaotic.

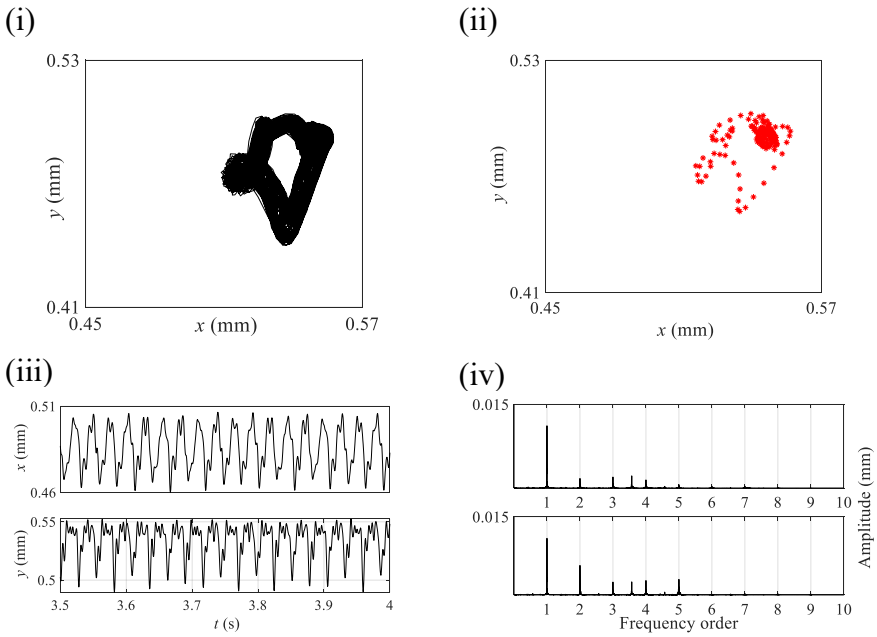

Figure 3 Experimental result of rotating machine at speed 37 Hz; (i) orbit plot, (ii) Poincare's map, (iii) time waveform, and (iv) FFT.

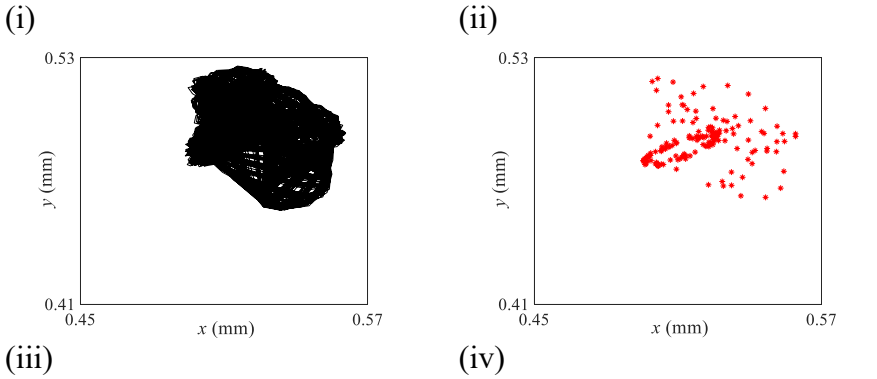

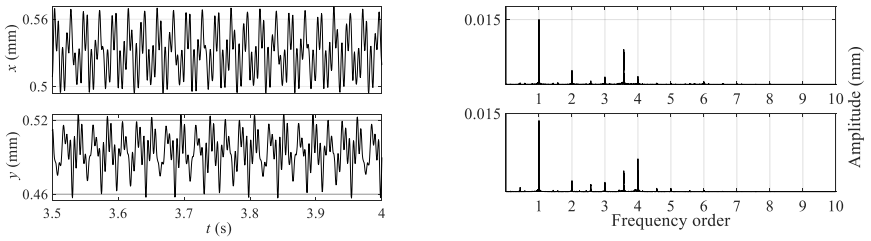

Figure 4 Experimental result of rotating machine at speed 45 Hz; (i) orbit plot, (ii) Poincare's map, (iii) time waveform, and (iv) FFT.

While the rotating speed is adjusted to 47 Hz, the trajectories exhibit random impact between the rotor and the stator (see Fig. 5). This random rub-impact is described as violent and dense. The spectra in Fig. 5iii indicate the sub-harmonic component (1/2x) and the fractional super-harmonic components (3/2x, 5/2x, 7/2x, 9/2x) with very small amplitudes. Also, Poincaré's map (Fig. 5ii) contains random attractors, thus the rub characteristic between the rotor and the stator is chaotic. It can be inferred from this result that the system has strong nonlinearity and complex dynamics due to the rubbing fault. Where a small increase in the running speed, totally changes the dynamic behavior of the rotor system.

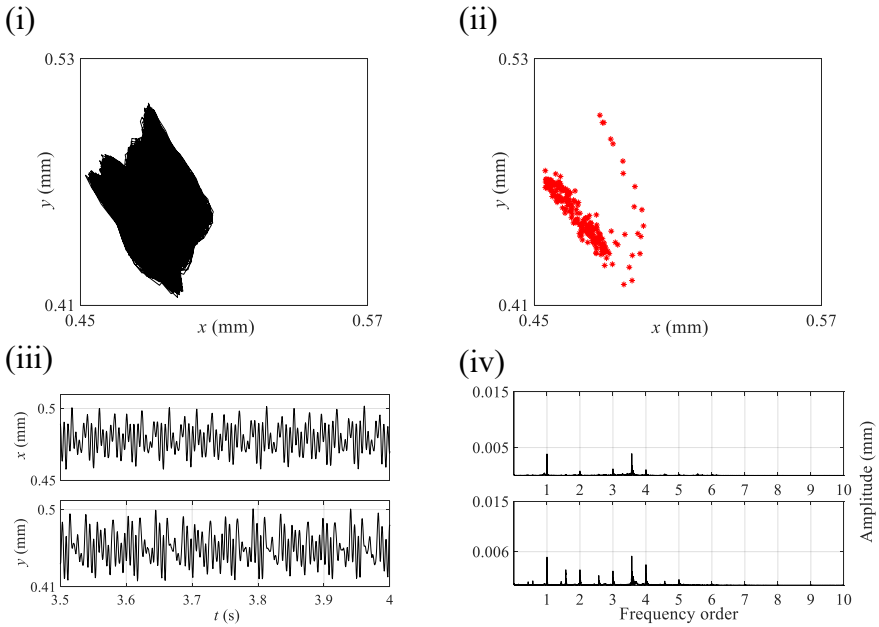

Figure 5 Experimental result of rotating machine at speed 47 Hz; (i) orbit plot, (ii) Poincare's map, (iii) time waveform, and (iv) FFT.

On the other hand, when rotating speed is adjusted to 51 Hz, the rub fault intensity is changed to serious chaotic behavior, as shown in (Figs. 6i, 6ii and 6iii). The frequency spectra illustrate a low amplitude of 1x harmonic component, especially in the vertical direction (see Fig. 6iv). Also, distinctive frequencies appear between harmonics (3x, and 7/2x).

In summary, referring to the previous results, it can be highlighted that the lateral vibration is significantly influenced by increasing the rotational speed. Generally, the impact is chaotic and its intensity increases rapidly from light to heavy chaotic with the increase of the rotational speed.

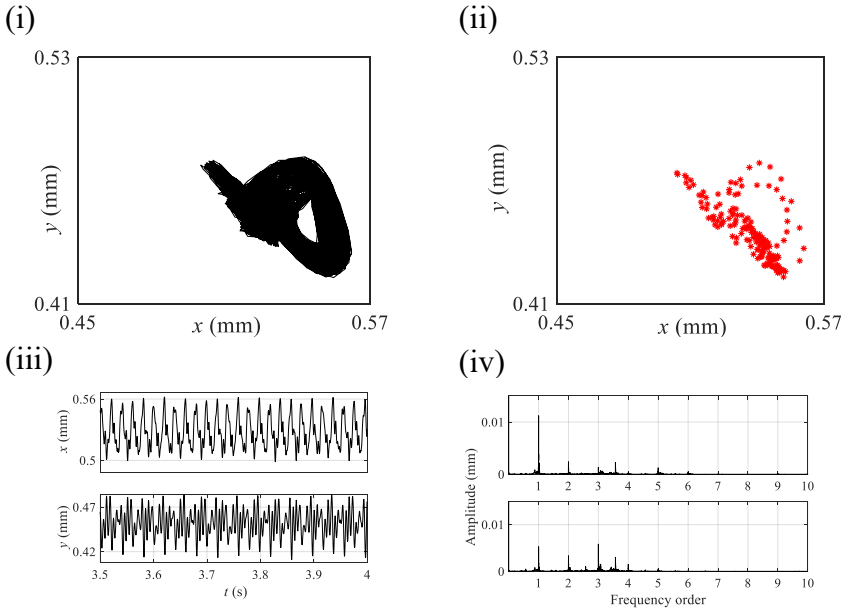

Figure 6 Experimental result of rotating machine at speed 51 Hz; (i) orbit plot, (ii) Poincare's map, (iii) time waveform, and (iv) FFT.

4. Conclusion

In this paper, the contact phenomenon due to lateral vibration of a simulated drill string is shown experimentally. The orbit plot, Poincare's map, FFT spectra, and time waveforms are used to discuss the characteristics of the rub fault. Based on the experimental results, It can be inferred that all rub responses are chaotic, and the chaotic intensity changes from slight to serious condition. The running speed

has an essential effect on the whirling motion of the drill string system. When the running speed is increased, the chaotic behavior becomes more voilent and intense. The orbit plot serve as a good graphical tool to monitor the influence of speed on the rub characteristics. The obtained FFT spectra of the measured signals show fractional sub-harmonic and super-harmonics frequency components. As the rub fault causes a strong nonlinearity in the rotating system, it can be observed changing the operating speed will result in complex dynamic behavior.

5. References

1. Xie, D., Z. Huang, Y. Ma, V. Vaziri, M. Kapitaniak, and M. Wiercigroch, *Nonlinear dynamics of lump mass model of drill-string in horizontal well.* International Journal of Mechanical Sciences, 2020. **174**. p. 105450.0020-7403.
2. Dong, G. and P. Chen, *A review of the evaluation, control, and application technologies for drill string vibrations and shocks in oil and gas well.* Shock and Vibration, 2016. **2016**
3. Kapitaniak, M., V. Vaziri, J.P. Chávez, and M. Wiercigroch, *Experimental studies of forward and backward whirls of drill-string.* Mechanical Systems and Signal Processing, 2018. **100**. p. 454-465.0888-3270.
4. Christoforou, A. and A. Yigit, *Dynamic modelling of rotating drillstrings with borehole interactions.* Journal of Sound and Vibration, 1997. **206**(2). p. 243-260.0022-460X.
5. Jansen, J., *Non-linear rotor dynamics as applied to oilwell drillstring vibrations.* Journal of Sound and Vibration, 1991. **147**(1). p. 115-135.0022-460X.
6. Javidi, M., M. Saeedikhani, and R. Omidi, *Failure analysis of a gas well tubing due to corrosion: a case study.* Journal of Failure Analysis and Prevention, 2012. **12**. p. 550-557.1547-7029.
7. Al-Hiddabi, S.A., B. Samanta, and A. Seibi, *Non-linear control of torsional and bending vibrations of oilwell drillstrings.* Journal of Sound and Vibration, 2003. **265**(2). p. 401-415.0022-460X.
8. de Moraes, L.P.P. and M.A. Savi, *Drill-string vibration analysis considering an axial-torsional-lateral nonsmooth model.* Journal of Sound and Vibration, 2019. **438**. p. 220-237.0022-460X.
9. Khulief, Y., F. Al-Sulaiman, and S. Bashmal, *Vibration analysis of drillstrings with string—borehole interaction.* Proceedings of the Institution of Mechanical Engineers, Part C: Journal of Mechanical Engineering Science, 2008. **222**(11). p. 2099-2110.0954-4062.
10. Nandakumar, K. and M. Wiercigroch, *Stability analysis of a state dependent delayed, coupled two DOF model of drill-stringvibration.* Journal of Sound and Vibration, 2013. **332**(10). p. 2575-2592.0022-460X.
11. Chávez, J.P., V.V. Hamaneh, and M. Wiercigroch, *Modelling and experimental verification of an asymmetric Jeffcott rotor with radial clearance.* Journal of Sound and Vibration, 2015. **334**. p. 86-97.0022-460X.
12. Yu, F., G. Huang, W. Li, H. Ni, B. Huang, J. Li, and J. Duan, *Modeling lateral vibration of bottom hole assembly using Cosserat theory and laboratory experiment verification.* Geoenergy Science and Engineering, 2023. **222**. p. 211359.2949-8910.

13. Spanos, P.D., A.M. Chevallier, N.P. Politis, and M.L. Payne, *Oil and gas well drilling: a vibrations perspective.* The Shock and Vibration Digest, 2003. **35**(2). p. 85-103.0583-1024.
14. Ghasemloonia, A., D.G. Rideout, and S.D. Butt, *A review of drillstring vibration modeling and suppression methods.* Journal of Petroleum Science and Engineering, 2015. **131**. p. 150-164.0920-4105.
15. Tiwari, R., *Rotor systems: analysis and identification*. 2018, Talyor and Fransic Group, New york: CRC press.
16. Kapitaniak, M., V. Vaziri, J. Páez Chávez, and M. Wiercigroch, *Numerical study of forward and backward whirling of drill-string.* Journal of Computational and Nonlinear Dynamics, 2017. **12**(6).1555-1415.
17. Lin, T., Q. Zhang, Z. Lian, Z. Xiao, T. Wang, G. Li, and J. Ding, *Experimental study on vibrational behaviors of horizontal drillstring.* Journal of Petroleum Science and Engineering, 2018. **164**. p. 311-319.0920-4105.
18. Zamani, S.M., S.A. Hassanzadeh-Tabrizi, and H. Sharifi, *Failure analysis of drill pipe: A review.* Engineering Failure Analysis, 2016. **59**. p. 605-623.1350-6307.
19. Chen, S.L., K. Blackwood, and E. Lamine, *Field investigation of the effects of stick-slip, lateral, and whirl vibrations on roller-cone bit performance.* SPE drilling & completion, 2002. **17**(01). p. 15-20.1064-6671.
20. Albdiry, M.T. and M.F. Almensory, *Failure analysis of drillstring in petroleum industry: a review.* Engineering Failure Analysis, 2016. **65**. p. 74-85.1350-6307.
21. Srivastava, S. and C. Teodoriu, *An extensive review of laboratory scaled experimental setups for studying drill string vibrations and the way forward.* Journal of Petroleum Science and Engineering, 2019. **182**. p. 106272.0920-4105.
22. Chu, F. and W. Lu, *Experimental observation of nonlinear vibrations in a rub-impact rotor system.* Journal of Sound and Vibration, 2005. **283**(3-5). p. 621-643.0022-460X.
23. Liao, C.-M., B. Balachandran, M. Karkoub, and Y.L. Abdel-Magid, *Drill-string dynamics: reduced-order models and experimental studies.* Journal of Vibration and Acoustics, 2011. **133**(4).1048-9002.
24. Liu, Y., T. Ma, P. Chen, and C. Yang, *Method and apparatus for monitoring of downhole dynamic drag and torque of drill-string in horizontal wells.* Journal of Petroleum Science and Engineering, 2018. **164**. p. 320-332.0920-4105.
25. Tian, J., Y. Yang, and L. Yang, *Vibration characteristics analysis and experimental study of horizontal drill string with wellbore random friction force.* Archive of applied mechanics, 2017. **87**. p. 1439-1451.0939-1533.
26. Abdo, J., E.M. Hassan, K. Boulbrachene, and J.C.T. Kwak, *Drillstring Failure—Identification, Modeling, and Experimental Characterization.* ASCE-ASME

Journal of Risk and Uncertainty in Engineering Systems, Part B: Mechanical Engineering, 2019. **5**(2). p. 021004.2332-9017.

27. Tian, J., L. Wei, and T. Zhang, *Dynamic research and experimental analysis of a new downhole drilling tool.* Arabian Journal for Science and Engineering, 2019. **44**. p. 10231-10244.2193-567X.
28. Choy, F.K., J. Padovan, and J.C. Yu, *Full rubs, bouncing and quasi chaotic orbits in rotating equipment.* Journal of the Franklin Institute, 1990. **327**(1). p. 25-47.0016-0032.